ESA STUDY CONTRACT REPORT

ESA Contract No:	SUBJECT:	CONTRACTOR:
21646/08/NL/NR	Generation of Mars Express / MARSIS Derived Enhanced Ionospheric Calibration Data	The Centre National de la Recherche Scientifique (CNRS)
* ESA CR( )No:	**No. of Volumes:** *3* **This is Volume No:** *1* Ionospheric Impact on MARSIS Radar Signal	**CONTRACTOR'S REFERENCE:** 3, rue Michel Ange F-75794 Cedex 16 France

ABSTRACT:

A planetary ionosphere is a perturbing environment for radar waves. Unfortunately, it is an unavoidable obstacle along the propagation path of signals emitting by orbiting radar sounders. The Mars Advanced Radar for Subsurface and Ionospheric Sounding (MARSIS) is an instrument onboard the European Space Agency's Mars Express spacecraft. In order to deeply penetrate the surface, MARSIS operates at MHz frequencies for which the perturbations due the Martian ionosphere can be significant. Therefore, prior to any analyze, MARSIS data need to be corrected from the ionospheric effects.

The aim of this document is to characterize the impact of the Martian ionosphere on MARSIS radar signals. This impact is a combination of three effects: Global absorption, phase distortion, and Faraday rotation. They are quantitatively described in the context of the ionized Martian environment and at MARSIS frequencies. Their relative disturbances on the received echoes are explained and discussed.

Name(s) of author(s):

Cyril Grima / LPG BP 53 - 38041 Grenoble Cedex 9 - France / cyril.grima@obs.ujf-grenoble.fr
Wlodek Kofman / LPG BP 53 - 38041 Grenoble Cedex 9 – France / wlodek.kofman@obs.ujf_grenoble.fr

** NAME OF ESA STUDY MANAGER:	** ESA BUDGET HEADING:
DIV: DIRECTORATE:	

* Sections to be completed by ESA
** Information to be provided by ESA Study Manager

Table of contents

1. **Introduction …… 2**
2. **The MARSIS instrument …… 3**
3. **The ionosphere …… 3**

3.1. Presentation …… **3**

3.2. The Electron density (N_e) …… **3**

3.3. The total electron content (TEC) …… **4**

3.4. The plasma frequency (f_p) …… **5**

3.5. The refractive index (n) …… **6**

3.6. The collision frequency (ν) …… **6**

4. **The impact of the ionosphere on MARSIS radar signal …… 7**

4.1. Global absorption …… **7**

4.2. Phase distortion …… **8**

4.3. Faraday rotation …… **9**

5. **Conclusion …… 9**
6. **References …… 13**

1. Introduction

The Mars Advanced Radar for Subsurface and Ionospheric Sounding (MARSIS) is an instrument of the Italian space Agency (ASI) [*Picardi et al.*, 2005]. It is orbiting onboard the Mars Express (MEX) spacecraft of the European Space Agency (ESA). MARSIS is getting data since its unfolding in the early summer 2005. Its primary science objective is to study the subsurface of Mars at a low-frequency regime to penetrate deep under the soil. The orbit of MEX is highly elliptical with a periapsis of 270 km and an apoapsis of 11600 km, thus always above the ionosphere. The ionosphere is a plasma which disturbs radio waves passing through it. Since MARSIS is an active instrument, it emits its own signal, which is backscattered by surface and subsurface structures before to be collected back. That is, along is propagation path, a MARSIS signal is two times disturbed by the ionosphere. In the final purpose of correcting the MARSIS data from the impact of the ionosphere, we characterize in this document the different ionospheric effects on the received echoes. Preliminary, we briefly present the MARSIS radar. We also describe important features of the Martian ionosphere, in order to get all the ionospheric parameters needed to study the impact of the ionosphere at MARSIS wavelengths.

2. The MARSIS instrument

MARSIS can operate in 2 different sounding modes. The first is a passive mode (receive only) called 'active ionospheric sounding' (AIS) [*Gurnett et al.*, 2005]. It sounds the ionosphere with a quasi-wave tone by swapping 160 frequencies in the range of 0.1 to 5.5 MHz. Of course, for the purpose of this document the ASI mode is not valuable. We will only focused on the second sounding mode, which study the subsurface with the active component of the radar (transmit and receive). MARSIS can use this subsurface sounding mode when the spacecraft is lower than 900 km. This represents 26 minutes of operation by orbit. It uses 4 different frequency bands centered to 1.8, 3, 4, and 5 MHz. Each band is 1 MHz wide. MARSIS operates in two bands simultaneously, in order to get the backscattered echoes as a function of the frequency. The choice of the two operating bands aims to minimize the impact of the ionosphere. It depends of the solar zenith angle (SZA) which is directly linked to the ionosphere activity. The MARSIS signal is emitted at a rate of 127.27 pulses per second. The returned pulses are integrated over 1 s to increase the signal-to-noise ratio (SNR). This final process gives an along-track resolution in the range of 5 to 9 km, varying with MEX altitude and speed. At this time the MARSIS coverage of Mars is almost complete.

3. The ionosphere

3.1. Presentation.

An ionosphere is mainly due to the ionization of the neutral upper atmosphere of Mars by sun radiation (photoionization). Since Mars is not shielded by a global magnetosphere as on earth, the solar wind and precipitations of particles also contribute as a source of ionization (impact ionization) [*Luhmann*, 1990; *Luhmann and Brace*, 1991]. Therefore, the sun is the main responsible and the ionosphere would be at a maximum intensity near the sub solar point (SZA = 0°), and decreases toward the terminator (SZA = 90°). Ideally, the ionosphere could be considered as nonexistent in the night side of the planet. On the day side the ionosphere becomes significant above 100 km in altitude.

Here after, we describe important features of the Martian ionosphere, in order to get all the ionospheric parameters needed to study the impact of the ionosphere at MARSIS wavelengths.

3.2. The electron density (N_e).

Although the ionosphere is an ionized medium, it remains globally neutral. That is there are as many positive charges that negative charges. So-considered, one can understand that the electron density is commonly used as a valid indicator for the global ionosphere density. Fig. 1 shows two MGS profiles obtained during the day for a normal ionosphere activity, and corresponding to a 2.7 MHz peak plasma frequency. The Mariner 6 profile corresponds to a high solar activity period, which can be considered as a high electron density case. The nocturnal profile was obtained by Mariner and Viking orbiters over the night side; its corresponding peak plasma frequency is 600 kHz. Our study will use those profiles as reference cases.

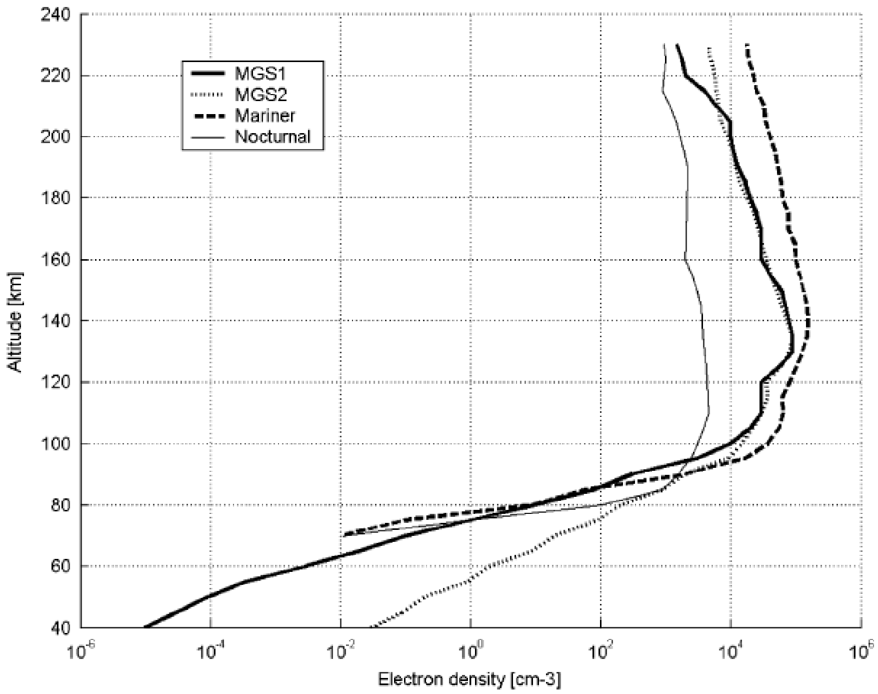

Fig. 1. Three samples of electron density for Mars based on data collected by Mariner and MGS missions (see text for details). The ionosphere is significant above 100 km in altitude. Note that values fewer than 90 km were extrapolated [from *Safaeinili and al.*, 2003]

3.3. The Total Electron Content (TEC).

One of the most important parameter of an ionosphere is the integral of electron density within a column of this ionosphere. This is called the total electron content and expressed in m^{-2} for a reference altitude. The Chapman model is generally used to describe the electron density profiles for different SZA [*Chapman*, 1931] with the following expression

$$N_e(z,\chi) = N_0 exp\left[0.5\left(1 - \frac{z-z_0}{H} - Ch\left(\frac{R_m+z_0}{H},\chi\right).exp\left(-\frac{z-z_0}{H}\right)\right)\right] \qquad (1)$$

where $N_e(z)$ is the electron density changing with the altitude z, N_0 is the maximum of the electron density, z_0 is the altitude of maximum of production of ionization, H is the height scale of the atmosphere, χ is the SZA, and *Ch()* is the Chapman incidence function [see *Chapman*, 1931].

The TEC on Mars has been measured as a function of the SZA by several experiments in orbit, included MARSIS [*Safaeinili et al.*, 2007; *Mouginot et al.*, 2008]. Those results are presented on Fig. 2, and show that the ionosphere is negligible just after the terminator at SZA = 100°.

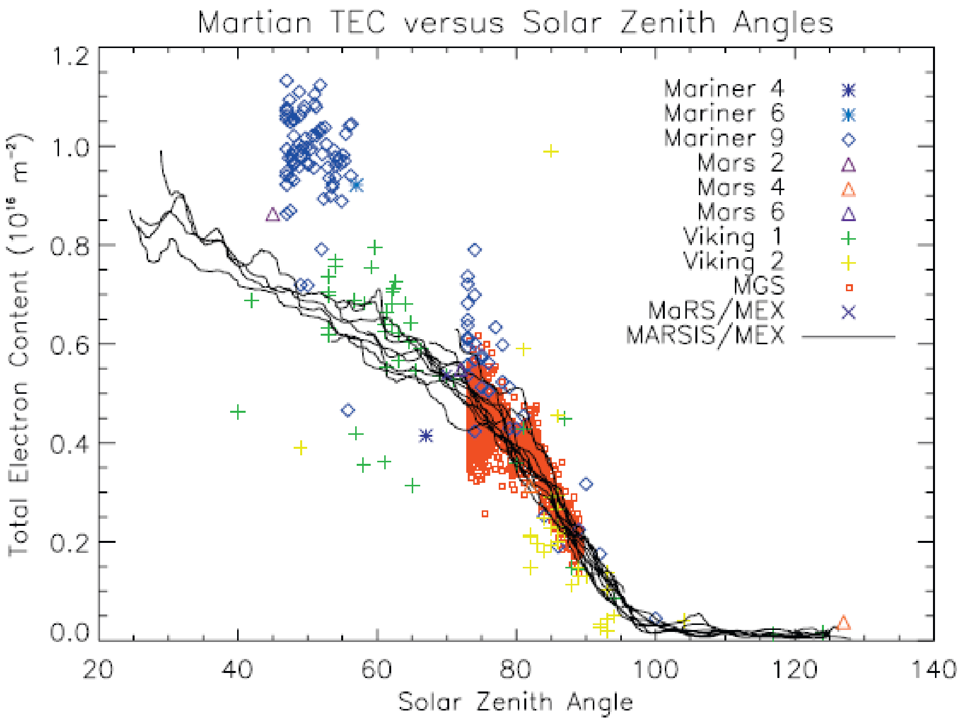

Fig. 2. Total electron content as a function of the sun zenith angle. Values are plotted from MARSIS, Mariner 4, 6, 9, Mars 2, 4, 6, Viking 1, 2, MGS, and MaRS/MEX. The TEC decreases toward the terminator, and the ionosphere is negligible after SZA = 100° [from *Mouginot et al.*, 2007].

3.4. The plasma frequency (f_p).

Independently from the magnetic field, the plasma frequency characterizes the plasma oscillations. It results from charge-density perturbations in the ionosphere. The plasma frequency is given by

$$f_p = \frac{q_e}{2\pi\sqrt{\varepsilon_0 m_e}}\sqrt{N_e} \approx 8.98\sqrt{N_e} \qquad (2)$$

where f_p is the plasma frequency, q_e is the electron charge, m_e is the electron mass, and ε_0 is the free space permittivity.

3.5. The refractive index (n).

A plasma has its own refractive index which depends both of the plasma frequency and the frequency of the wave crossing it. The refractive index is given by *Budden* [1964]

$$n = \sqrt{1 - \frac{\omega_p^2}{\omega^2}} \approx 1 - \frac{1}{2}\left(\frac{\omega_p^2}{\omega^2}\right) - \frac{1}{8}\left(\frac{\omega_p^2}{\omega^2}\right)^2 - \frac{1}{16}\left(\frac{\omega_p^2}{\omega^2}\right)^3 \quad (3)$$

where n is the refractive index, ω_p is the plasma pulsation and $\omega = 2\pi f$ is the wave pulsation of the radio signal. For the purpose of our future work, we developed n to the third order. *Mouginot et al.* [2008] has shown this development to be a sufficient approximation. Note that a signal could no propagate in the ionosphere if its frequency is lower than the plasma frequency.

3.6. The collision frequency (ν)

The average rate of collision between particles in the ionosphere is described by the collision frequency. Different formulas lead to this value,

Melnik's formula [*Melnik and Parrot*, 1999]:

$$\nu(Hz) = 2.12 \times 10^{-16} N_n(m^{-3}) T_e^{1/2} \quad (4)$$

Schunk's formula [*Schunk and Nagy*, 1980]:

$$\nu(Hz) = 3.68 \times 10^{-14} N_{CO2}(m^{-3})[1 + 4.1 \times 10^{-11} \times |4500 - T_e|^{2.93}] \quad (5)$$

where $\nu(Hz)$ is the collision frequency, N_n is the neutral density, N_{CO2} is the carbon dioxide density, and T_e is the electronic temperature. Although one of these formula used N_n and the other N_{CO2}, they gives both very similar results since neutral particles of the Martian ionosphere are mainly carbon dioxide ones.

Fig. 3 shows different collision frequency profiles as a function of the altitude, obtained with diurnal particle densities. The 'Melnik' and 'Schunk' profiles were plotted with the corresponding formulas, while the used electronic temperature and density profiles were extracted from *Melnik and Parrot* [1999]. The 'Witasse' profile is an application of the Schunk's formula with the values of *Mc Cormick and Whitten* [1990]. Thus, those profiles were obtained using different set of values and formulas. Despite this, the results are very similar and show how reliable could be the available estimations for the collision frequency.

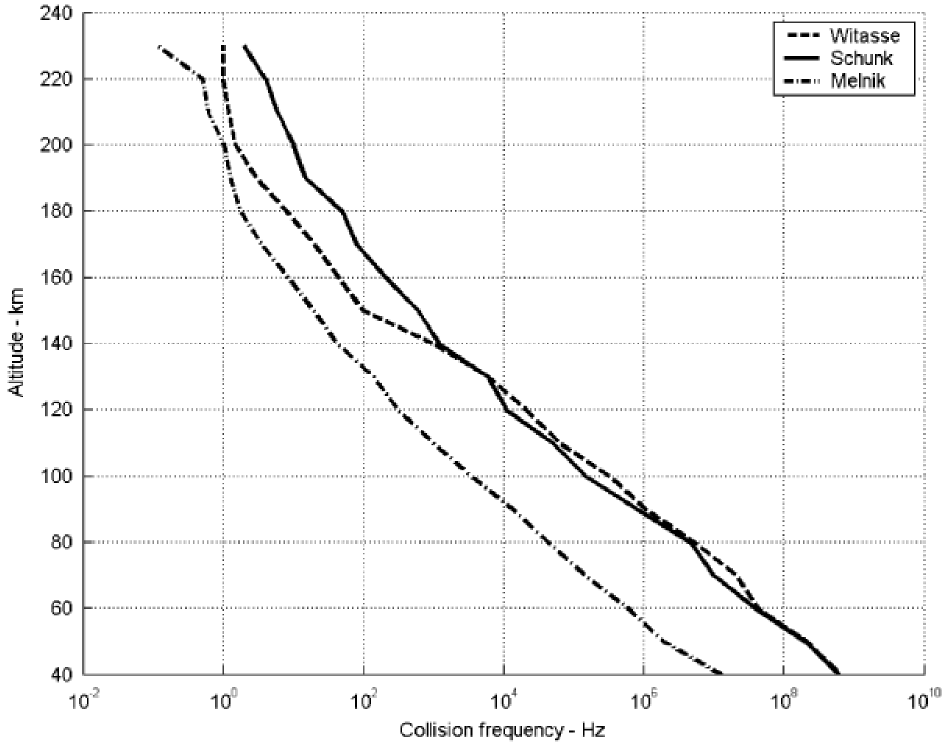

Fig. 3. Collision frequency dependence on altitude. See text for details. [From *Safaeinili et al.*, 2003]

4. The impact of the ionosphere on MARSIS radar signal

In the previous part of this document, several parameters of the ionosphere of Mars were detailed for different conditions (e.g. diurnal, nocturnal, high solar activity), and at MARSIS wavelengths. We will now use those values to estimate the impact of the ionosphere, which is a combination of three different effects: Global absorption, phase distortion, and Faraday rotation.

4.1. Global absorption

As in any medium, a radio wave is naturally attenuated as it is traversing the ionosphere. This absorption is given by *Safaeinili et al.* [2007]

$$\alpha(dB/km) = \frac{10{,}000\log(e)}{c}\left(1 - \frac{\omega_p^2}{\omega^2}\frac{2\omega^2-\omega_p^2}{\omega^2-v^2}\right)^{0.25}\frac{v\omega_p^2}{\omega^2+v^2-\omega_p^2} \tag{6}$$

where v is the collision frequency. In general $v^2 << \omega^2$. Furthermore, if we assume $\omega_p << \omega$, this equation can be reduce to

$$\alpha(\omega) = 4.61 \times 10^4 N_e \frac{v}{\omega^2} \tag{7}$$

Thus, a one-way absorption could be written

$$\alpha(\omega) = \frac{4.61 \times 10^4}{\omega^2} \int_0^{H_{SC}} N_e(z) v(z) dz \tag{8}$$

where H_{sc} is the spacecraft altitude. In Fig. 4, attenuation as a function of the frequency is plotted for different conditions. The nocturnal profile shows the attenuation to be very low compared to the 4 MARSIS bands. During the day, the higher MARSIS bands (3, 4 and 5 MHz) have tolerable absorption.

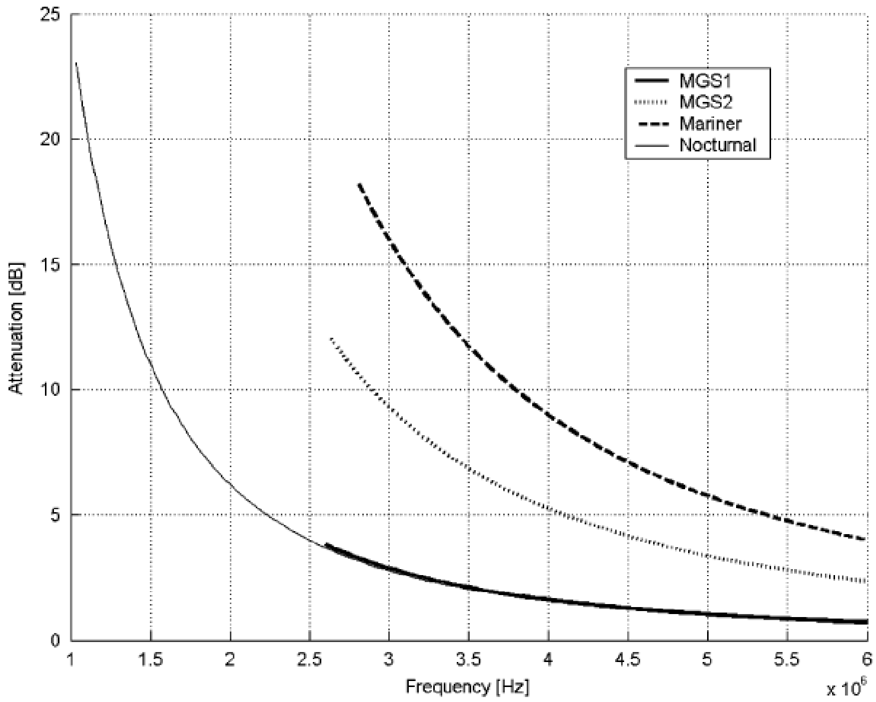

Fig. 4. Total attenuation due to one-way ionospheric propagation [From *Safaeinili et al.*, 2003]

4.2. Phase distortion

Previously, we see that the refractive index of the ionosphere depends on the radio frequency. Since a MARSIS pulse is emitted over a 1 MHz bandwidth, it will be affected in an anisotropic fashion by the ionosphere. This implies a delay and a spreading of the pulse, which are both a consequence of the phase distortion of the signal by reference to in-vacuum propagation [*Budden*, 1964; *Safaeinili et al.*, 2003]

$$\Delta\varphi(\omega) = \frac{2\omega}{c} \int_{h_1}^{h_2} \Re(n-1)\,.\,dz \tag{9}$$

where $\Delta\varphi$ is the phase distortion. Using Eqs. (2) and (3), *Mouginot et al.* [2008] rewrite Eq. (9) as

$$\Delta\varphi(f) = \frac{a_1}{f} + \frac{a_2}{f^3} + \frac{a_3}{f^5} \tag{10}$$

defined by the terms

$$a_1 = 40.32 \times \int N_e^1(h).dz \times \frac{4\pi}{c} \tag{11.1}$$

$$a_2 = 812.851 \times \int N_e^2(h).dz \times \frac{4\pi}{c} \tag{11.4}$$

$$a_3 = 32774.2 \times \int N_e^3(h).dz \times \frac{4\pi}{c} \tag{11.3}$$

Fig. 5 is a simulation of this phase distortion on a MARSIS pulse at 5MHz (the higher MARSIS band), with and without ionosphere. The delay and the spreading are obvious, and show how the phase distortion needs to be corrected for a good use of the data.

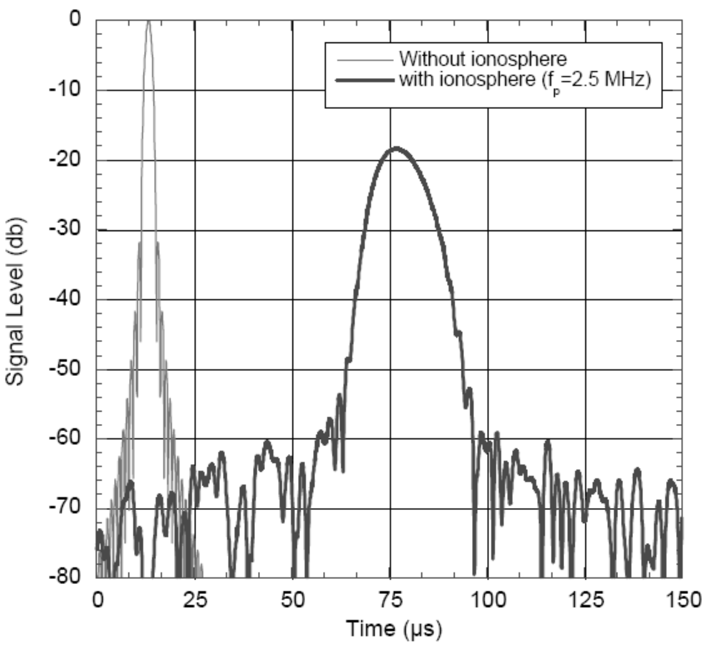

Fig. 5. A radar echo without and with ionosphere (f_p=2.5 MHz). The radar carrier frequency is 5 MHz. [From *Safaeinili et al.*, 2003]

4.3. Faraday rotation

A radio wave will be attenuated and slowed by the presence of a magnetic field along the propagation path. A remnant magnetic field printed in the Martian crust has been attested by Acuña et al. [1999]. The field is more frequent in the older southern hemisphere. Though it can locally reach 1500 nT, 80% of Mars has a magnetic field strength of less than 50 nT. Fig. 6 shows the global distribution of the crustal magnetic field over Mars, and Fig. 7 highlights its hemispheric asymmetry.

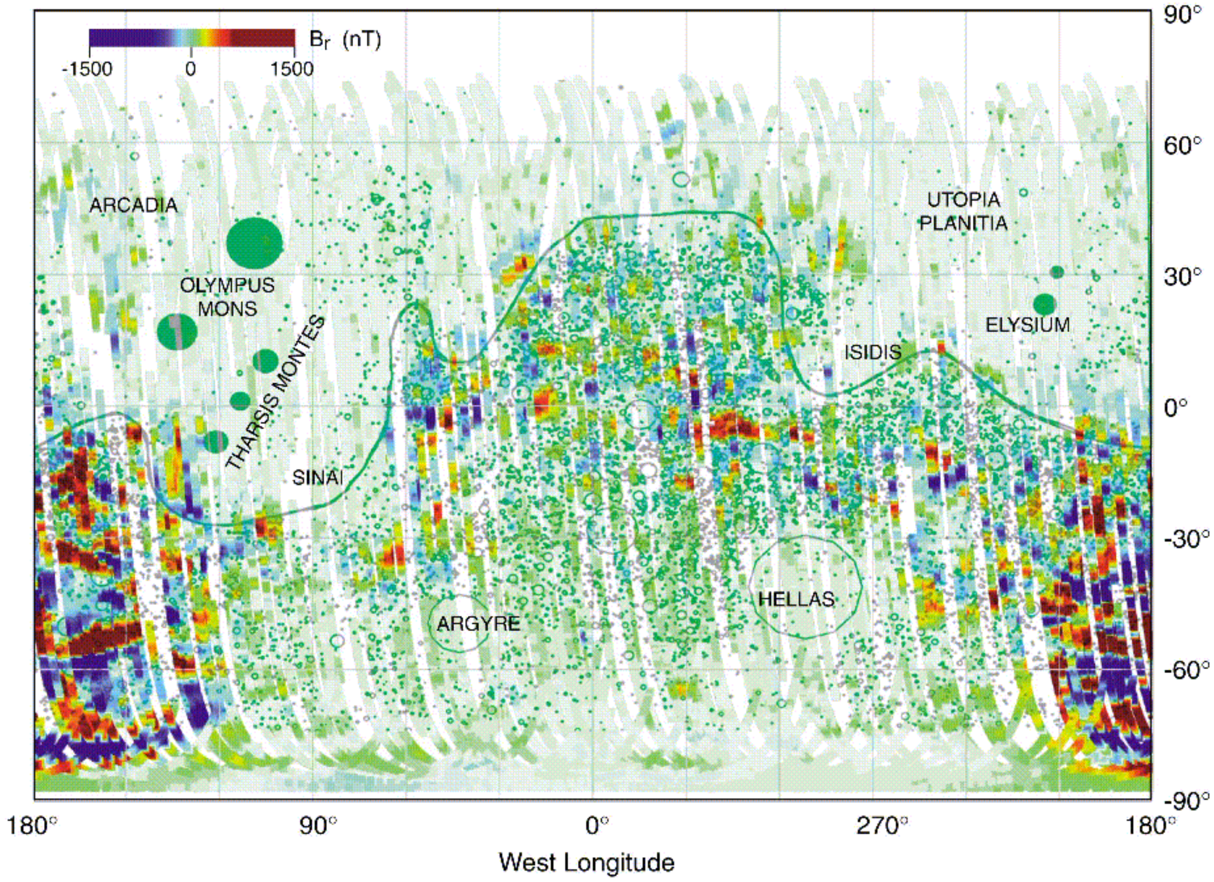

Fig. 6. Map showing the distribution of crustal magnetic field sources on a map showing the distribution of craters greater than 15 km in diameter and the dichotomy boundary (solid line). [From *Acuña et al.*, 1999]

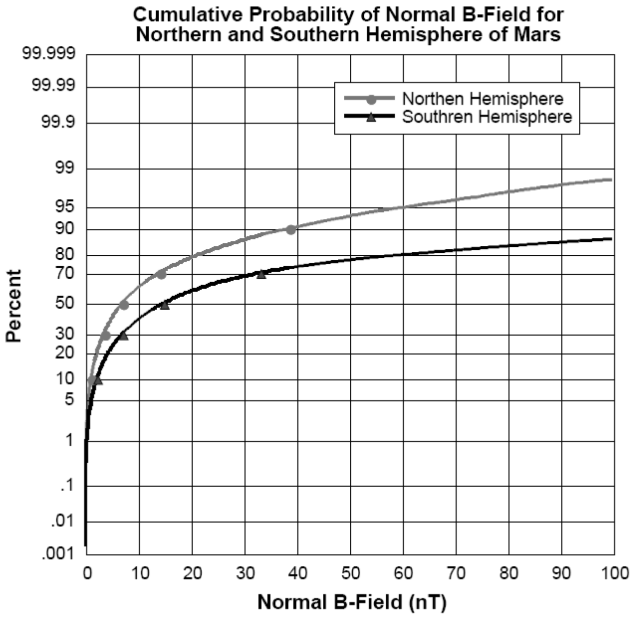

Fig. 7. Cumulative probability distribution of the normal component of the magnetic field for the northern and southern hemisphere of Mars [From *Safaeinili et al.*, 2003].

Eq. (3) gives the refractive index of the ionosphere without magnetic field. In the presence of a magnetic field, we should introduce the cyclotron frequency of an electron. For a circularly polarized wave, the refractive index of the medium becomes

$$n_{\pm} = \sqrt{1 - \frac{\omega_p^2}{\omega(\omega \pm \omega_c)}} \tag{12}$$

with

$$\omega_c = \frac{q_e}{m_e} B \tag{13}$$

where ω_c is the cyclotron frequency of an electron, q_e is the electron charge, m_e is the electron mass, and B is the magnetic field normal to the motion of the electron. Since $\omega_c \ll \omega$, the ionospheric attenuation is usually the same as Eq. (3), except for high magnetic fields. The decomposition of the linear polarization wave into two circularly polarized waves leads *Safaeinili et al.* [2003] to write the one-way polarization angle rotation as

$$\frac{d\Psi}{dz} = \frac{k}{2}\left(n_+(z) - n_-(z)\right) \tag{14}$$

where k is the wave number, and after approximation

$$\frac{d\Psi}{dz} = \frac{q_e}{2m_e c} \frac{\omega_p^2(z) B_n}{\omega\sqrt{\omega^2 - \omega_p^2(z)}} \quad (15)$$

The total polarization angle along the propagation path is then

$$\Psi = \frac{k}{2}\int_0^h (n_+(z) - n_-(z)).dz$$

$$= 9.33 \times 10^5 \frac{B_n}{\omega^2}\left(\int_h^h n_{e(z)} dz + \frac{1591.8}{\omega^2}\int_0^h n_e^2\,(z) dz\right)$$

$$\approx 9.33 \times 10^5 \frac{B_n}{\omega^2} TEC \quad (16)$$

Fig.8 shows the delay effect on the radio signal. As one can see, only the case with a very high magnetic field could imply a slight effect at MARSIS wavelengths, and in Martian conditions. In Fig. 9, the round-trip Faraday rotation is plotted as a function of the frequency. One should note that only a rotation close to 90° or its odd multiples would cause a significant fading of the signal. Therefore, the attenuation will be important only under very worst conditions, at large magnetic field and daytime operation.

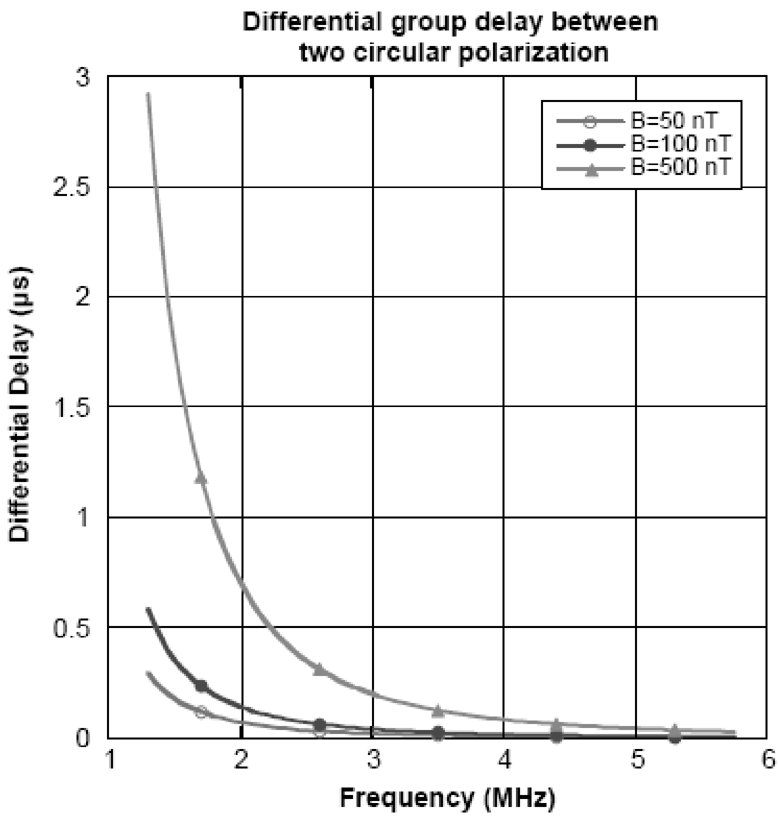

Fig. 8. Differential group delays for two circular waves with opposite polarization for three different magnetic field strengths [From *Safaeinili et al.*, 2003].

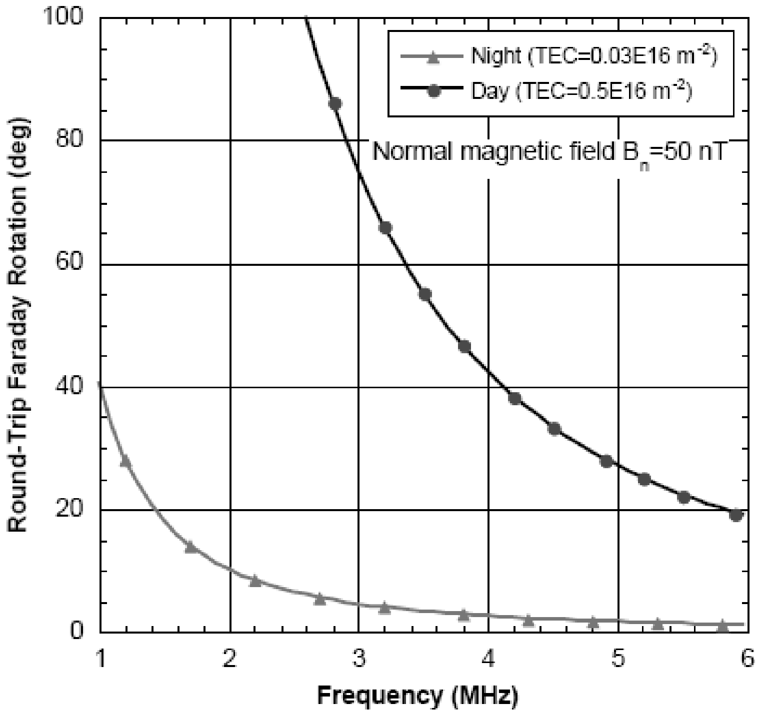

Fig. 9. Faraday rotation for a case where the peak plasma frequency is 1 MHz with a profile similar to the one shown in Fig. 1 and a radial magnetic field intensity of 50 nT [From *Safaeinili et al.*, 2003].

5. Conclusions

Because the radio frequencies are close to the plasma frequency of the ionosphere, one should correct the impact of the ionosphere on the MARSIS radar signal before any analyses of the subsurface data. The three main ionospheric effects disturbing the radio signal propagation were analyzed. 1) The global attenuation can be neglected during the night, while the use of the three higher bands should avoid a significant absorption on the day side (SZA < 90°). 2) The two consequences of the phase distortion (delay and spreading of the pulse) are over all dominant on diurnal conditions. They should be corrected before any analyses of the signal. 3) The remnant magnetic field of Mars could produce a slight delay of the pulse over the few local high magnetic anomalies in the southern hemisphere, but this could be partially avoiding by using the higher MARSIS bands. Likewise, the induced Faraday rotation will not have any significant effect over more than 80% of the Martian surface where the magnetic field is lower than 50 nT.

6. References

Acuña, M.H., Connerney, J.E.P., Ness, N.F., Lin, R.P., etal. 1999. Global distribution of crustal magnetization discovered by Mars global surveyor MAG/ER experiment. *Science 284*, 790-793.

Budden, K.G. 1964. Lectures on magnetoionoc theory. Gordon & Breach Publishing Group, London.

Chapman, S.. 1931. Absorption and dissociative or ionizing effects of monochromatic radiation in an atmosphere on a rotating earth. *Proc. Soc. London 43,* 1047-1055.

Gurnett, D.A., Kirchner, D.L., Huff, R.L., Morgan, D.D., et al. 2005. Radar soundings of the ionosphere of Mars. *Science 310*, 1929-1933.

Luhmann, J.G. 1990. The solar wind interaction with unmagnetized planets: a tutorial. *Geophys. Mono. 58*, 401-411.

Luhmann, J.G., and Brace, L.H. 1991. Near-Mars space. *Rev. Geophys. 29*, 121-140.

Mc Cormick, P.T., Whitten, R.C. 1990. The dynamics of the ionosphere of Mars at large solar zenith angle*. J. Geophys. Res. 95*, 6263

Melnik, O., and Parrot, M.. 1999. Propagation of electromagnetic waves through the Martian ionosphere. *J. Geophys. Res. 104*, 12705.

Mouginot, J., Kofman, W., Safaeinili, A., and Herique, A. 2008. Correction of the Ionospheric distortion on the MARSIS surface sounding echoes. *Planet. Space Sci. 56*, 917-926.

Picardi, G., Plaut, J.J., Biccari, D., Bombaci, O., et al. 2005. Radar soundings of the subsurface of Mars. *Science 310*, 1925-1928.

Safaeinili, A., Kofman, W., Nouvel, J-F, Herique, A., and Jordan, R.L. 2003. Impact of Mars ionosphere on orbital radar sounder operation and data processing. *Planet. Space Sci. 51*, 505-515.

Safaeinili, A., Kofman, W., Mouginot, J., Gim, Y., et al. 2007. Estimation of the total electron content of the Martian ionosphere using radar sounder surface echoes. *Geophys. Res. Lett. 31*, doi:10.1029/2007GL032154.

Schunk, R.W., and Nagy, A.F. 1980. Ionospheres of terrestrial planets. *Rev. Geophys. Space Phys. 18*, 813.